IOP Conf. Series: Materials Science and Engineering **330** (2018) 012048 doi:10.1088/1757-899X/330/1/012048

Dissimilar Joining of Stainless Steel and 5083 Aluminum Alloy Sheets by Gas Tungsten Arc Welding-Brazing Process

Muralimohan Cheepu[1]*, B. Srinivas[2], Nalluri Abhishek[2], T. Ramachandraiah[3], Sivaji Karna[4], D. Venkateswarlu[5]

[1]Department of Mechatronics Engineering, Kyungsung University, Busan 48434, Republic of Korea.
[2]Department of Mechanical Engineering, MVGR College of Engineering, Andhra Pradesh 535005, India.
[3]Senior Engineer, Department of Research and Development, D&H Secheron Electrodes Pvt. Limited, Madhya Pradesh 452006, India.
[4]Defence Research and Development Laboratory, Telangana 500058, India.
[5]Department of Mechanical Engineering, Marri Laxman Reddy Institute of Technology and Management, Telangana 500043, India.

Email: *muralicheepu@gmail.com

Abstract. The dissimilar joining using gas tungsten arc welding - brazing of 304 stainless steel to 5083 Al alloy had been conducted with the addition of Al-Cu eutectic filler metal. The interface microstructure formation between filler metal and substrates, and spreading of the filler metal were studied. The interface microstructure between filler metal and aluminum alloy characterized that the formation of pores and elongated grains with the initiation of micro cracks. The spreading of the liquid braze filler on stainless steel side packed the edges and appeared as convex shape, whereas a concave shape has been formed on aluminum side. The major compounds formed at the fusion zone interface were determined by using X-ray diffraction techniques and energy-dispersive X-ray spectroscopy analysis. The micro hardness at the weld interfaces found to be higher than the substrates owing to the presence of Fe_2Al_5 and $CuAl_2$ intermetallic compounds. The maximum tensile strength of the weld joints was about 95 MPa, and the tensile fracture occurred at heat affected zone on weak material of the aluminum side and/or at stainless steel/weld seam interface along intermetallic layer. The interface formation and its effect on mechanical properties of the welds during gas tungsten arc welding–brazing has been discussed.

1. Introduction

In recent years, the joining of light weight dissimilar materials is becoming increasingly demand in the manufacturing of hybrid structures and sub components for various industrial applications. The selection of materials combination for hybrid structures are depending on their strength, density and metallurgical properties. The light weight metals such as aluminum and magnesium, which have excellent corrosion resistance and high specific-strength. Due to their tremendous properties, the importance of these materials towards lightweight construction in the transportation and chemical industries has led increased to achieve the aim of versatility of the equipment [1]. However, these materials alone cannot withstand the required properties for specific applications. To meet their requirements the hybrid column structures of aluminum alloy to stainless steel has a great interest among enormous industrial applications. Conversely, the joining between stainless steel and aluminum alloy has difficulties using conventional arc welding techniques due to the formation of brittle intermetallic compounds in the fusion zone [2-5]. To make successful joining between these dissimilar materials solid state welding methods such as friction stir [6], friction welding [7-13] have been contemplated. Other than the joining problems, these processes are having several issues of making welds of different joint designs, length and type of joints. Besides the solid state joining processes a new techniques have been developed using arc welding processes of gas metal arc welding (GMAW) and gas tungsten arc welding (GTAW) with low heat input method using different fluxes [14]. The researchers studied the joining of these dissimilar metals successfully by using of new techniques with the tungsten inert gas welding (TIG) - brazing then this processes act as a welding joint on aluminum side and steel side joint is same as a brazing joint [15].

Most recently this welding method (tungsten inert gas welding-brazing technique) increased an interest as a major development field in welding of steel and lightweight aluminum alloys. In this technique, substrates and melting of consumable fillers are melted by TIG arc, and then joint can be formed. As stated earlier in conventional fusion welding processes the liquid filler metal cannot wet and spread as a brazing filler on any surface of the steel. To improve the liquid metal wetting angle of the fillers on substrate surfaces previous studies reported that the noncorrosive flux can increase the liquid meal wetting angle of fillers in Al brazing and the molten flux easily adhere to the aluminum hot dip galvanized steel surface [16,17]. However, all these processes are involved in development of intermetallic phases owing to the interaction time between substrates and filler metal, the solid surface dissolves into filler metal. In general the intermetallic compounds are more brittle and it will limits the mechanical properties of the joints when their thickness at interface exceeds more than the permissible value. Most of the research reports available on cold metal transfer or laser arc brazing of aluminum alloys to steel [18]. Furthermore, in this study the dissimilar material joining of butt joint using gas tungsten arc welding – brazing of 304 stainless steel and 5083 Al alloy with the addition of Al-Cu eutectic filler metal. The weldments were analysed with their seam formation on aluminum side and steel side, its microstructure and tensile strength of the joints, and crack formation issues were discussed.

2. Experimental Procedure

In the present work, the AA5083 alloy with a thickness of 3 mm and 304 stainless steel (304 SS) (2 mm thickness) were used as base materials. The filler meal used was 2319 Al-Cu welding wires diameter of 1.2 mm was used. The chemical composition of the base metals used for this work are shown in Table 1. The welding process of gas tungsten arc welding - brazing was done using Esab weld skill 200 HF welding power source and 15 l/min flow rate of pure argon was selected as shielding gas. The base metals were machined into the size of 120x60 mm and the surfaces were polished with emery paper and followed by cleaning with acetone before starting the welding experiment. The thin sheets were prepared with V-groove shape with an angle of 30˚ in aluminum alloy side and 40˚ in stainless steel side. The welding parameters were optimized by trial and error method with varying the various parameters, and the optimal parameters of distance of 3 mm between electrode tip to substrate and a travel speed of 110 mm/min were kept constant with varying welding current from 95 A to 180 A. During welding copper was used as a backing plate, and the Al-Cu filler metal was inserted to the weld pool to make the GTAW-brazing joints. The schematic view of the GTAW-brazing of stainless steel to aluminum is shown in figure 1. After completion of welding, the weldments were cut in transverse direction to prepare the metallographic samples for microstructural evolution and defects analysis. The weldments were etched with two different etchants such as Keller's etchant solution (HCl 1.5 ml + HF 1 ml + HNO_3 2.5 ml + H_2O 95ml) in aluminum side and Vilella's etchant solution (C_2H_6O 100 ml + picric acid 1g + HCl 5 ml). The microstructures of the welds were examined under optical microscope, and chemical composition of the weld interfaces were analysed through scanning electron microscope (SEM) and energy dispersive X-ray spectroscope (EDS). Micro hardness was conducted across the weld joint and mechanical tensile properties of the welds were tested using universal tensile machine, at a 1 mm/min cross head speed. The tensile samples were prepared as per the ASTM E8 standard [19], and maximum values of the tensile strength were taken from the average of three samples.

Table 1 Chemical composition of the base metals used for the present study

5083 Aluminum	Mn	Mg	Fe	Si	Ti	Cr	Cu	Zn	Al
	0.49	4.25	0.38	0.28	0.13	0.18	0.08	0.09	balance
304 Stainless steel	C	Mn	P	Si	S	Cr	Ni	N	Fe
	0.06	1.89	0.036	0.025	0.69	18.1	8.2	0.08	balance

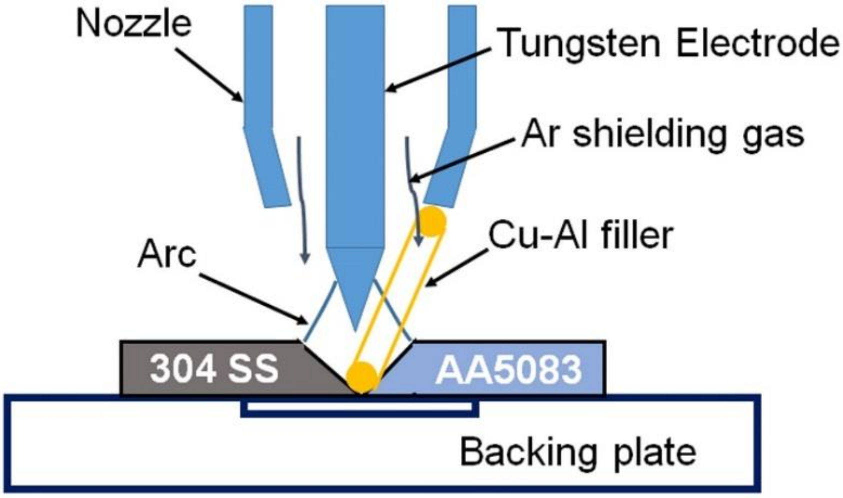

Figure 1 Schematic view of the GTAW-brazing used for stainless steel and aluminum joining

3. Results and Discussions

The spreading of molten filler metal behavior of on the substrate groove faces has influence on the welding of stainless to aluminum with GTA welding – brazing process [20]. The wetting behavior of the filler metal with substrates is different with change in welding current. To understand this phenomena, welding has been performed using different welding currents. For all welding currents with in the selected conditions, a smooth and good shape of weld same was made. Joints made at low welding current values are resulted in unfilled face of the weld seam, whereas the joints formed with the filling weld seam face and root for the welding currents above 100 A. This may be associated to the different degree of weld seam temperature with increasing current, the greater the melting of the used filler metal and improves in wettability of the molten filler metal with the stainless steel. The resulted welds revealed that the weld seams are clean and are free from the formation any slag particles, which are commonly produced in gas metal arc welding [21-23]. The macrostructures of the joints exhibited the aluminum side which has low melting temperature is alike welding joint whilst stainless side observed that there is no melting occurred and a thin reaction layer is formed between the molten filler and groove surface. The microstructures of joints across the seam interfaces and aluminum side are illustrated in figure 2. Most of the studies were reported on evaluation of the interfaces between weld seam and stainless steel side with the formation of intermetallic compound [3,14]. Song *et al*. [15] and Zhang *et al*. [24], have been reported that the interface of welded seam/stainless steel appeared with three different intermetallic layers. These intermetallic layers varied in thick with respect to temperatures and location of the weld joint. They also investigated that the top of the groove characterized with the formation of thick intermetallic layers with the size of 20 μm which is thicker than the other locations of the joint. The similar observations are found for the weld interface of weld seam and stainless steel characterized with unequal thickness of intermetallic layer formation along the weld interface. Whereas, the interface of weld seam to aluminum is also critical issue on the joint formation. The interface properties drastically varying with the welding current,

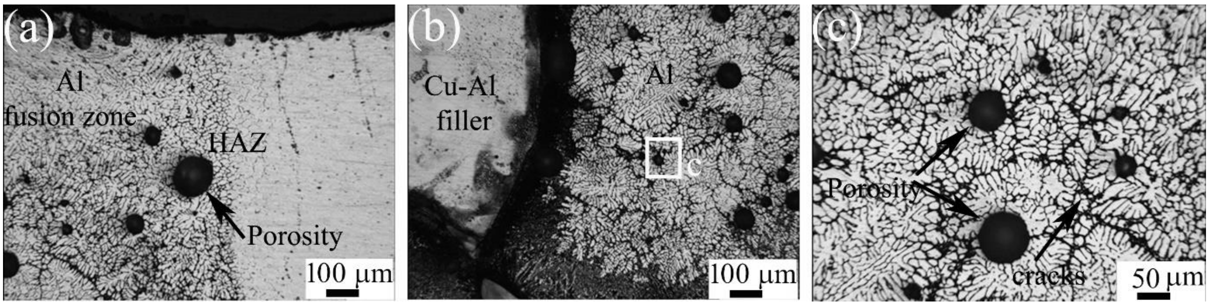

Figure 2 Microstructures of the joints showing (a) HAZ aluminum side (b) interface of aluminum and Al-Cu filler and (c) Porosity formation on aluminum side

welding procedure, and an easy to form the defects on aluminum side. Due to the variation in melting temperatures of the substrates, aluminum side always results in sensitive microstructural formation. The width of HAZ on aluminum side increasing with increasing welding current, and it is observed that the formation of porosity for joints made at higher welding currents (see fig 2a). The other side of joint interface of weld seam and aluminum is always depending on the filler metal composition and type of fillers using for arc brazing [25]. It is observed that the formation of micro cracks for joints made at low welding currents (see fig 2b), and the magnified view of microstructure is in clear that exhibits the microstructural cracks and pores adjacent to the weld interface. It is also found that the offset of the electrode has influence on the filling of molten filler and HAZ formation on aluminum side (an extensive study on this phenomenon is not indicated in this study). SEM-EDS analysis was carried out on the joint interfaces to identify the formation of phases of the intermetallic compounds. The chemical content of the stainless steel/weld seam interface identified that of Al (69.54-71.24 at. %), Fe (18.21-21.98 at. %) and that of Cr (5.65-6.24 at. %) and Ni (1.54-1.08 at.%) is indicates the formation of Fe_2Al_5 compounds. Whereas, the interface of aluminum/weld seam indicates the content of Al (79.84-85.21 at. %) and Cu (16.95-13.54 at. %) which is identified as Al_2Cu phase [15,18,24].

Vickers micro-hardness of the weld seam and joint interfaces were measured, is shown in figure 3, it is identified that the hardness rapidly increased in the interface of the joint. The interface of the stainless steel/weld seam is obtained highest hardness with an average value of 602 HV and hardness of weld seam/aluminum interface is found to be an average value of 264 HV. The existence of such a high hardness indicates the presence of intermetallic compounds which can make the joint very brittle and deteriorates the efficiency and mechanical strength of the joints. The joints tensile strength under tensile loads indicates that joints strength is distinct at altered welding currents, is illustrated in figure 4. The joint strength gradually differs when the operating welding currents in between 95 A, and 125 A, and the average values of joints of maximum strength of 95 MPa at 140 A. The strength of the final joint comparatively lower at 95 A, since the formation of incomplete brazing caused to low heat input thus results in lower temperature at joint interface, which will control the improper formation of spreading and wetting of the molten filler metal, hence instigating of poor mechanical properties. On the contrary, it is observed that the higher welding currents produces heat input level also higher, thus ensued in a further decreasing of tensile strength due to the high temperature at weld interface owing to the extreme melting of the filler metal and aluminum. The inter solubility and reactions between the Fe, Al and Cu elements there is possibility of formation of weld cracking at the joint interfaces which lowers the joints strength. To confirm the presence of intermetallic compounds across the tensile fractured faces/paths under tensile tests, the tensile fractured surfaces were characterized with XRD analysis, are shown in figure 5. It is confirmed that the joint fracture surfaces contained Fe_2Al_5, Fe_4Al_{13} and $CuAl_2$ phases. The brittle nature of these intermetallic compounds of the weld interface limited the mechanical resistance of the welds and event at low tensile forces it could easily fractured especially its thickness exceeds the threshold limit value which is about 10 μm [26,27]. The SEM observations of the fractured surfaces were examined that the coarse dimples morphology formation representing the ductile nature of fracture. It is also observed that there are few dark gray spots appearing along the fracture path, and are associated

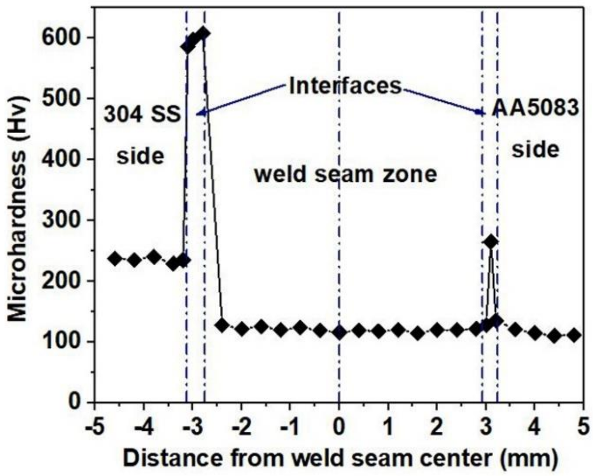

Figure 3 Micro-hardness distribution across the joint interfaces

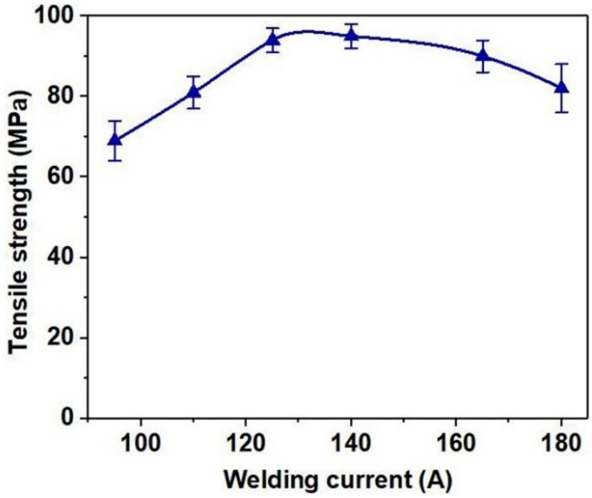

Figure 4 Tensile strength of the joints at different welding currents

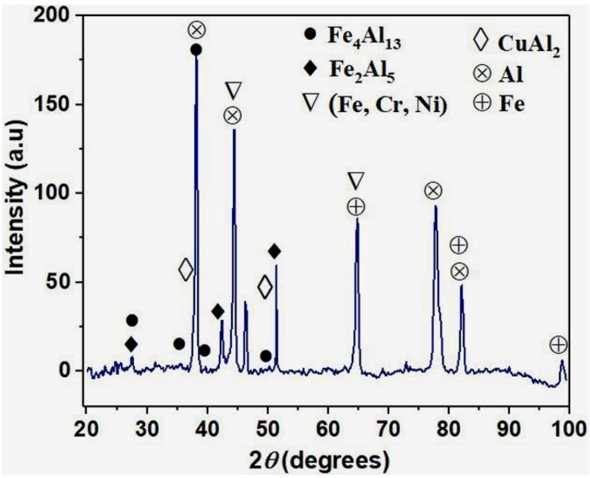

Figure 5 X-ray diffraction analysis showing the formation of phases in fracture surfaces

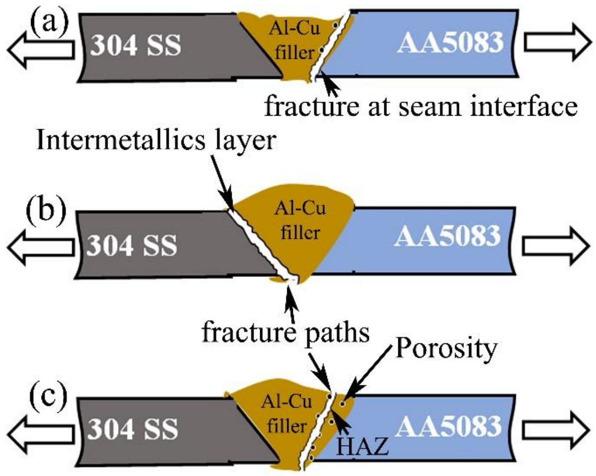

Figure 6 Fracture path of the joints under tensile loads at welding currents of (a) 95 A, (b) 140 A and (c) 180 A

with the brittle intermetallic compounds. The presence of these phases along the interfaces will impair the tensile strength, and also change the fracture path under tensile loads. There are three kinds of tensile fractures observed for the joints, and these are varying with different welding currents. The existence of various fracture paths between the weld seam and substrates are depicted in figure 6. As explained earlier lower welding currents resulted in lower interface temperatures, thus the occurrence of fracture taken place along the weld seam/aluminum interface owing to the improper bonding formation [28-32]. Whereas, the second type of fracture occurred along the intermetallic layer which is formed in stainless streel/weld seam interface. The fracture initiated from the top of the weld seam where the intermetallic layer is thicker compared to other locations of the joint. On the contrary, third type of fracture initiated from the micro cracks and porosity in the aluminum side fusion zone and propagated into the HAZ of the aluminum. The maximum strength obtained for the joints where the fracture exists along the intermetallic layers at stainless steel/weld seam interface.

4. Conclusions

The dissimilar joining of stainless steel to 5083 aluminum alloys were butt welded using GTA welding - brazing with the addition of Cu-Al filler metal. The spreading behavior of shows the molten filler differs with the different welding currents. At lower welding currents an incomplete joint seem was formed, whereas an excellent weld seam formation was obtained with the complete filling of weld face and root for the optimum welding currents. The maximum strength of 95 MPa achieved for the joints attained for optimum conditions. The joints at higher welding currents exhibited the defects formation and a molten welding joint between aluminum and weld seam interface. The tensile fracture of the joints occurred at stainless steel/weld seam interface along the intermetallic layer (Fe_2Al_5, Fe_4Al_{13} and $CuAl_2$) for which the joints acquired the maximum tensile strength.

References

[1] Kah P, Suoranta R, Martikainen J and Magnus C 2014 Techniques for joining dissimilar materials: metals and polymers *Rev. Adv. Mater. Sci.* **36** 152-64.

[2] Muralimohan C H, Ashfaq M, Ashiri R, Muthupandi V and Sivaprasad K 2016 Analysis and characterization of the role of Ni interlayer in the friction welding of titanium and 304 austenitic stainless steel *Metall. Mater. Trans. A.* **47** 347-59.

[3] Song J L, Lin S B, Yang C L, Fan C L and Ma G C 2010 Analysis of intermetallic layer in dissimilar TIG welding–brazing butt joint of aluminium alloy to stainless steel *Sci. Technol. Weld. Join.* **15** 213-18.

[4] Cheepu M, Ashfaq M and Muthupandi V 2017 A new approach for using interlayer and analysis of the friction welding of titanium to stainless steel *Trans. Indian. Inst. Met.* **70** 2591-600. https://doi.org/10.1007/s12666-017-1114-x

[5] Cheepu M M, Muthupandi V and Loganathan S 2012 Friction welding of titanium to 304 stainless steel with electroplated nickel interlayer *Mater. Sci. Forum.* **710** 620-25.

[6] Kimapong K and Watanabe T 2004 Friction stir welding of aluminum alloy to steel *Weld. J.* 277-82.

[7] Cheepu M, Muthupandi V, Srinivas B and Sivaprasad K 2018 Development of a friction welded bimetallic joints between titanium and 304 austenitic stainless steel *Techno-Societal 2016, International Conference on Advanced Technologies for Societal Applications ICATSA 2016 ed Pawar P M, Ronge B P, Balasubramaniam R and Seshabhattar S (Springer, Cham) Chapter 73* 709-17. https://doi.org/10.1007/978-3-319-53556-2_73

[8] Muralimohan C H, Haribabu S, Reddy Y H, Muthupandi V and Sivaprasad K 2014 Evaluation of microstructures and mechanical properties of dissimilar materials by friction welding *Procedia. Mater. Sci.* **5** 1107-13.

[9] Muralimohan C H, Haribabu S, Reddy Y H, Muthupandi V and Sivaprasad K 2015 Joining of AISI 1040 steel to 6082-T6 aluminium alloy by friction welding *J. Adv. Mech. Eng. Sci.* **1(1)** 57-64. http://dx.doi.org/10.18831/james.in/2015011006

[10] Kimura M, Ishii H. Kusaka M. Kaizu K.and Fuji A 2009 Joining phenomena and joint strength of friction welded joint between pure aluminium and low carbon steel *Sci. Technol. Weld. Join.* 14 388-95.

[11] Muralimohan C H, Muthupandi V and Sivaprasad K 2014 The influence of aluminium intermediate layer in dissimilar friction welds *Inter. J. Mater. Res.* **105** 350-57.

[12] Muralimohan C H, Muthupandi V and Sivaprasad K 2014 Properties of friction welding titanium-stainless steel joints with a nickel interlayer *Procedia. Mater. Sci.* **5** 1120-29.

[13] Muralimohan C H and Muthupandi V 2013 Friction welding of type 304 stainless steel to CP titanium using nickel interlayer *Adv. Mater. Res.***794** 351-57.

[14] He H, Wu C, Xie Z, Liu Y, Xu W and Jing Y 2017 Effects of alloyed fluxes on spreading behavior and microstructures of aluminum–titanium TIG brazing interface *Metallogr. Microstruct. Anal.* **6** 82-8.

[15] Song J L, Lin S B, Yang C L, Ma G C and Liu H 2009 Spreading behavior and microstructure characteristics of dissimilar metals TIG welding–brazing of aluminum alloy to stainless steel, *Mater. Sci. Eng. A.* **509** 31-40.
[16] Roulin M, Luster J W, Karadenz G and Mortensen A 1999 Strength and structure of furnace-brazed joints between aluminum and stainless steel *Weld. J.* **78** 151-55.
[17] Peyre P, Sierra G, Beaume F D, Stuart D and Fras G 2007 Generation of aluminium-steel joints with laser-induced reactive wetting *Mater. Sci. Eng. A.* **444** 327-38.
[18] Zhang H T, Feng J C, He P and Hackl H 2007 Interfacial microstructure and mechanical properties of aluminium-zinc-coated steel joints made by a modified metal inert gas welding-brazing process *Mater. Charact.* **58** 588-92.
[19] ASTM E8 / E8M-16a, Standard test methods for tension testing of metallic materials, ASTM International, West Conshohocken, PA, 2016, www.astm.org.
[20] Cole G S and Sherman A M 1995 Lightweight materials for automotive applications, *Materials. Characterization.* **35** 3-9.
[21] Ahsan M R U, Cheepu M, Ashiri R, Kim T H, Jeong C and Park Y D 2017 Mechanisms of weld pool flow and slag formation location in cold metal transfer (CMT) gas metal arc welding (GMAW) *Weld. World.* **61** 1275-85. https://doi.org/10.1007/s40194-017-0489-y
[22] Muralimohan C H, Ahsan M R, Lim S S and Park Y D 2016 Slag control formation behavior of consumable electrodes in gas metal arc welding (GMAW) process *The Korean Society of Welding and Joining, 2016 Spring Conference* 2016.4 **64** 183-183.
[23] Cheepu M, Kim Tae Hoon, Park Joo Hyun and Park Yeong Do 2016 A study on the development of wires for reduction slag for MAG welding of automotive chassis parts *The Korean Society of Welding & Joining 2016 Fall Conference* 2016.11 **65** 94-94.
[24] Zhang Y, Huang J, Cheng Z, Ye Z, Chi H, Peng L and Chen S 2016 Study on MIG-TIG double-sided arc welding-brazing of aluminum and stainless steel *Mater. Lett.* **172** 146-48.
[25] Dong H, Hu W, Duan Y, Wang X and Dong C 2012 Dissimilar metal joining of aluminum alloy to galvanized steel with Al–Si, Al–Cu, Al–Si–Cu and Zn–Al filler wires *J. Mater. Process. Technol.* **212** 458-64.
[26] Weis S, Elßner M, Wielage B and Wagner G 2017 Wetting behavior of AlAgCu brazing filler on aluminum matrix composites and stainless steel *Weld. World.* **61** 383-89.
[27] Murugan S P, Cheepu M, Nam D G and Park Y D 2017 Weldability and fracture behaviour of low carbon steel/aluminium/stainless steel clad sheet with resistance spot welding *Trans. Indian. Inst. Met.* ***70*(3)** 759-68.
[28] Cheepu M, Muthupandi V and Che W S 2018 Improving mechanical properties of dissimilar material friction welds *Appl. Mech. Mater.* **877** 157-62. doi:10.4028/www.scientific.net/AMM.877.157
[29] Venkateswarulu D, Cheepu M, Krishnaja D and Muthukumaran S 2018 Influence of water cooling and post-weld ageing on mechanical and microstructural properties of the friction-stir welded 6061 aluminium alloy joints *Appl. Mech. Mater.* **877** 163-76. doi:10.4028/www.scientific.net/AMM.877.163
[30] Cheepu M, Haribabu S, Ramachandraiah T, Srinivas B, Venkateswarulu D, Karna S, Alapati S and Che W S 2018 Fabrication and analysis of accumulative roll bonding process between magnesium and aluminum multi-layers *Appl. Mech. Mater.* **877** 183-89. doi:10.4028/www.scientific.net/AMM.877.183
[31] Devireddy K, Devuri V, Cheepu M and Kumar B K 2018 Analysis of the influence of friction stir processing on gas tungsten arc welding of 2024 aluminum alloy weld zone *Int. J. Mech. Prod. Eng. Res. Dev.* **8(1)** 243-52. DOI: 10.24247/ijmperdfeb201828
[32] Cheepu M, Venkateswarlu D, Mahapatra M M and Che W S 2017 Influence of heat treatment conditions of Al-Cu aluminum alloy on mechanical properties of the friction stir welded joints. *Korean Welding and Joining Society*, **11**, 264-264. http://www.dbpia.co.kr/Journal/ArticleDetail/NODE07278590